IN VIVO QUANTIFICATION OF SPIO NANOPARTICLES FOR CELL LABELING BASED ON MR PHASE GRADIENT IMAGES

Luning Wang[1], William Potter[2], and Qun Zhao[1]

[1]*Department of Physics and Astronomy, University of Georgia, Athens, GA, United States,* [2]*Laboratory of Plasma Studies, Cornell University, Ithaca, NY, United States*

Target audience: Scientists and clinicians interested in quantification of iron oxide nanoparticles, susceptibility quantification, and phase gradients.

Purpose: Super-paramagnetic iron oxide (SPIO) nanoparticles have been widely used in magnetic resonance imaging (MRI), such as cell labeling [1]. At a high concentration, MR signal decays fast, posing challenges to quantify SPIO nanoparticles. The quantitative susceptibility mapping (QSM) method uses MR phase to quantify SPIO nanoparticles [2] and is less influenced by the signal loss. But the QSM method usually requires phase unwrapping, which is a nontrivial task. To avoid phase unwrapping, we propose a method to use phase gradients to quantify SPIO nanoparticles used for labeling C6 glioma cells.

Methods: Phase gradient images have been demonstrated to be continuous and smooth [3]. Here we propose a Fourier based method to calculate gradients of a wrapped phase: $\nabla_x\varphi = \cos\varphi \cdot FT^{-1}[k_x \cdot FT(\sin\varphi)] - \sin\varphi \cdot FT^{-1}[k_x \cdot FT(\cos\varphi)]$ (1). The derived phase gradient images will be further filtered using the spherical mean value (SMV) theorem to remove the background field [4]. Additionally, since phase perturbation is resulted from inhomogeneous susceptibility distribution [2], so the phase gradients can also be calculated by: $FT(\nabla_x\varphi) = -\gamma B_0 TE \sum_{n=1}^{N} \chi_n \cdot FT(V_n) \cdot [k_x \cdot (1/3 - k_z^2/k^2)]$ (2). In Eq. 2, we suppose that there exist N regions containing SPIO nanoparticles, χ_n is the susceptibility of the n^{th} region, and V_n represents the volume of the n^{th} region. A combination of Eqs. 1 and 2 enables an efficient quantification of susceptibilities of SPIO nanoparticles.

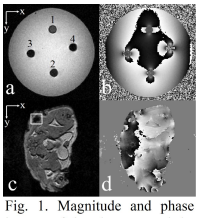

Fig. 1. Magnitude and phase images of the phantom and the mouse.

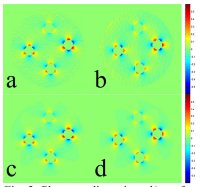

Fig. 2. Phase gradients in rad/mm for the phantom.

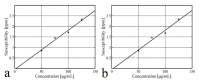

Fig. 3. Concentration vs. susceptibility.

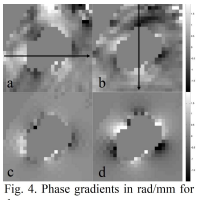

Fig. 4. Phase gradients in rad/mm for the mouse.

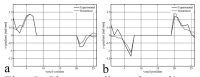

Fig. 5. Phase gradients in rad/mm along the two arrows in Fig. 4.

Phantom experiment: A phantom was made by using four vials of aqueous suspensions of SPIO nanoparticles (FerroTec, Santa Clara, CA), with the concentrations of 50, 75,100 and 125 μg/mL. The phantom was imaged on a 3 T GE Signa HDx scanner (GE healthcare, Waukesha, WI) using a 3D SPGR sequence (TR/TE = 1s/4.6 ms, θ = 30°, FOV = 14×14×9 cm^3, size = 128×128×90). The four vials were segmented based on the magnitude images, and the susceptibility of each vial was assumed as a constant.

In vivo experiment: About 1.1 × 10^6 C6 glioma cells (10^5 labeled and 10^6 unlabeled) were subcutaneously injected into the flank of a nude mouse. This procedure was repeated for four mice. After 1 to 3 days post-injections, the in vivo images were acquired on 3 T Philips Achieva scanner (Phillips Medical Systems, Best, Netherlands) using a 3D SPGR sequence (TR/TE = 12.6/4.6 ms, θ = 30°, FOV = 4×4×0.9 cm^3, and size = 256×256×16). This study was performed as part of an approved institutional animal care and use community protocol. The area containing C6 glioma cells was segmented from surrounding tissues based on MR magnitude images. Since susceptibility was not uniform in the area, thus based on the voxel intensities from low to high, the segmented region of C6 glioma cells were further divided into ten small regions, with each small region having the similar signal intensity. By assuming the susceptibility of each small region was a constant, the susceptibilities of the ten small regions were calculated using voxels near the C6 glioma cells. The averaged susceptibility (χ_{avg}) was derived using $\chi_{avg} = \sum_{i=1}^{10} m_i\chi_i \Big/ \sum_{i=1}^{10} m_i$, where m_i and χ_i are the number of voxels and the susceptibility of the i^{th} small region, respectively.

Results: Fig. 1 shows the magnitude and phase images of the phantom and a representative mouse. The four vials (labeled in Fig. 1(a)) and the C6 glioma cells (indicated in Fig. 1(c)) appeared darker than the surrounding agar gel and tissues. The phase wrapping artifacts are presented as fringes in Figs. 1(b) and (d). The x- and y-axes were labeled at the upper-left corner of Figs. 1(a) and (c).

Figs. 2(a) and (b) present the experimental x- and y-gradients of the phase image in Fig. 1(b). Unlike the wrapped phase, the phase gradients are smooth and continuous. The magnetic dipole pattern can be used as a marker to localize SPIO nanoparticles. Figs. 2(c) and (d) illustrate the calculated x- and y-gradients, with the blooming patterns similar to Figs. 2(a) and (b). To investigate the deviation between the experimental and calculated results, the R^2 values, derived using voxels close to the vials, are about 0.955 for Figs. 2(a) and (c), and 0.951 for Figs. 2(b) and (d), indicating the proposed method worked well for the phantom experiment. The quantified susceptibilities of the four vials were 0.85, 1.45, 1.71, and 2.32 ppm using the x-gradient, and, 0.85, 1.46, 1.69, and 2.33 ppm using the y-gradient. Then, the concentrations of SPIO nanoparticles were linearly fitted to the susceptibilities, as shown in Fig. 3. The slopes of the fitted lines for Figs. 4(a) and (b) are 0.0188 and 0.0187 ppm·mL/μg under a 3 T magnetic field.

Mouse	From x-gradient		From y-gradient		Average
	Susceptibility [ppm]	Concentration [μg/mL]	Susceptibility [ppm]	Concentration [μg/mL]	Concentration [μg/mL]
1	3.12	167	3.18	170	168.5
2	3.60	192	3.51	188	190.0
3	2.73	146	2.97	159	152.5
4	3.51	188	3.46	185	186.5

Table 1: Estimated susceptibilities and concentrations of the SPIO nanoparticles used for labeling the C6 glioma cells.

The phase gradient images of the C6 glioma cells were presented in Figs. 4(a) and (b). Magnetic dipole patterns can be observed surrounding the area containing the tumor cells. The calculated x- and y-gradients were illustrated in Figs. 4(c) and (d). Since the experimental results were also influenced by the anisotropic susceptibility property of tissues and the air-tissue boundary, mismatches between the experimental and calculated results can be observed in the figures, and the R^2 values are about 0.69 for Figs. 4(a) and (c), and 0.70 for Figs. 4(b) and (d), which reduces approximately 27% compared to the phantom study. To further investigate the proposed method, Figs. 5(a) and (b) illustrate the 1D profiles of the experimental (solid) and calculated (dotted) x- and y-gradients along the two arrows, crossing the middle of the injected cells, in Figs. 4(a) and (b). As shown, the dotted curves generally match the solid curves in the most part of the profiles, indicating fairly accurate quantifications of the SPIO nanoparticles. Table 1 enumerates the averaged susceptibilities of the areas containing C6 glioma cells for the four mice, which were converted into the concentrations of the SPIO nanoparticles used for cell labeling based on the phantom result. Table 1 shows that the concentrations estimated from the x- and y-gradients are consistent for the same mouse, but fluctuate slightly among different mice.

Discussion: As an important type of contrast agents, the SPIO nanoparticles have been utilized in various applications in MRI. In this study, we labeled the C6 glioma cells using the SPIO nanoparticles, and injected them into four nude mice. After 1 to 3 days' growth of the C6 glioma cells, we quantified the concentration of SPIO nanoparticles inside the regions of the C6 glioma cells by using the in vivo MR phase gradient images under 3 T magnetic field. Quantification was first calibrated using a phantom experiment, where data was acquired using the same echo time and magnetic field strength to generate similar phase gradients. The fluctuation of the concentrations of the SPIO nanoparticles among different mice indicates that many biological effects, such as migration and death of labeled cells, blood diffusions, aggregation of the labeling nanoparticles, may probably contribute to the dynamic change of the concentrations of both the injected cells and the SPIO nanoparticles [5]. Additional studies of the above-mentioned dynamic changes need to be conducted in the future.

Conclusion: A new method was proposed to quantify SPIO nanoparticles using MR phase gradients. Both the phantom and in vivo mouse experiments demonstrated that the concentration of SPIO nanoparticles could be determined in fair accuracy and consistency.

References: [1] Kustermann et al, Contrast media & molecular imaging 2008;3(1):27-37. [2] de Rochefort et al, MRM 2008;60(4):1003-1009. [3] Zhao et al, NMR in Biomed 2011;24(5):464-472. [4] Schweser et al, NeuroImage 2011;54(4):2789-2807. [5] Kotek et al, Contrast media & molecular imaging 2012;7(2):195-203.